PALEOCEANOGRAPHY, VOL. 12, NO. 2, PAGES 321-336, APRIL 1997

Coupled ocean-atmosphere model response to freshwater input: Comparison to Younger Dryas event

Syukuro Manabe and Ronald J. Stouffer

NOAA Geophysical Fluid Dynamics Laboratory, Princeton University, Princeton, New Jersey

Abstract. This study explores the responses of a coupled ocean-atmosphere model to the discharge of freshwater into the North Atlantic Ocean. In the first numerical experiment in which freshwater is discharged into high North Atlantic latitudes over a period of 500 years, the thermohaline circulation (THC) in the Atlantic Ocean weakens, reducing surface air temperature over the northern North Atlantic Ocean and Greenland and, to a lesser degree, over the Arctic Ocean, the Scandinavian peninsula, and the Circumpolar Ocean and the Antarctic continent of the southern hemisphere. Upon the termination of the water discharge at the 500th year, the THC begins to intensify, regaining its original intensity in a few hundred years. With the exception of the Pacific sector of the Circumpolar Ocean of the southern hemisphere, where the surface air temperature recovery is delayed, the climate of the northern North Atlantic and surrounding regions rapidly resumes its original distribution. The evolution of the ocean-atmosphere system described above resembles the Younger Dryas event as inferred from the comprehensive analysis of ice cores and deep-sea and lake sediments. In the second experiment, in which the same amount of freshwater is discharged into the subtropical North Atlantic again over a period of 500 years, the THC and climate evolve in a manner qualitatively similar to the first experiment. However, the magnitude of the THC response is 4-5 times smaller. It appears that freshwater is much less effective in weakening the THC if it were discharged outside high North Atlantic latitudes.

1. Introduction

The isotopic analysis of Greenland ice cores suggests that large and rapid changes of climate occurred frequently during the last glacial and postglacial periods. For example, the isotopic ($\delta_{18}O$) temperature dropped very rapidly approximately 13,000 years ago, followed by the so-called Younger Dryas event (Y-D) when the isotopic temperature was almost as low as the last glacial maximum. Faunal and palynological analyses indicate that during the period of the Y-D cooling, surface temperature was very low not only over the northern North Atlantic but also over western Europe. The cold Y-D period, which lasted several hundred years, ended abruptly, as indicated by the records from Greenland ice cores.

Broecker et al. [1985] suggested that these abrupt changes resulted from very rapid changes in thermohaline circulation (THC) from one mode of operation to another. They further speculated that meltwater from continental ice sheets caused the capping of the oceanic surface by relatively freshwater in high North Atlantic latitudes and was responsible for the rapid weakening of THC and abrupt cooling of climate.

Such a rapid cooling of climate occurred in a numerical experiment which was performed at the Geophysical Fluid Dynamics Laboratory of NOAA [*Manabe and Stouffer*, 1995]. In response to a massive, 10-year discharge of freshwater into the northern North Atlantic, the THC weakened very rapidly, lowering the temperatures of the northern North Atlantic and western Europe. Upon the suspension of the water discharge, the THC exhibits a complex transient behavior which consists of an abrupt increase and decrease, followed by a gradual recovery of the initial state. Their result indicates that when the onset and termination of the massive meltwater discharge is very abrupt, the THC could weaken and intensify very rapidly due to the sudden reduction and increase in the rate of the deep water formation, respectively. However, upon the termination of the water discharge, the THC reintensified rapidly and surface temperature returned to the original state.

The numerical experiment described above yielded a cold event lasting a few hundred years, which is much shorter than the ~1000 year duration of the Y-D event. In a numerical experiment conducted here, we have prolonged the cold period by discharging freshwater at a much slower rate but over a much longer period, 500 years, thereby creating the cooling event with the duration comparable to the Y-D.

It is likely that meltwater is most effective in reducing the deep water formation when it is discharged near the sinking region of the THC. *Broecker et al.* [1988] speculated that the diversion of meltwater from the Mississippi to the St. Lawrence River was responsible for the reduction of deep water formation during the Y-D. To evaluate the effectiveness of the high-latitude as compared with the low-latitude dis-

Paper number 96PA03932.

charge of meltwater for the weakening of the THC, we conducted a second numerical experiment in which freshwater was discharged into the subtropical rather than high latitudes of the North Atlantic Ocean.

It appears that the Y-D cooling occurred not only over the North Atlantic and surrounding regions, but also over various regions in the rest of the world. For example, a return of cold-climate vegetation to the central region of western Canada and Alaska [*Mathews et al.*, 1993; *Engstrom et al.*, 1990] and major advances of Franz Joseph glacier in the New Zealand Alps [*Denton and Hendy*, 1994] indicate that while much weaker than in the North Atlantic, the Y-D event was felt in many parts of the world. On the basis of careful analysis of the numerical experiments conducted here, this study will explore whether the weakening of the THC in the North Atlantic could induce such cooling in other parts of the world and will investigate the physical mechanisms responsible for such cooling.

Previously, many freshwater flux perturbation experiments [e.g., *Maier-Reimer and Mikolajewicz*, 1989; *Marotzke*, 1990: *Weaver and Sarachik*, 1991] were conducted using general circulation models (GCMs) of the oceans in which surface water flux was prescribed and sea surface temperature (SST) was restored toward the fixed surface air temperature with the time constant of ~1 month [*Haney*, 1971]. With such "mixed" boundary conditions, the THC in ocean models is very sensitive to the discharge of freshwater. For example, in the model of Marotzke, the THC collapsed in response to a very small perturbation of salinity which was less than the "great salinity anomaly" of the 1970s. *Zhang et al.* [1993] suggested that the extreme sensitivity of the THC noted above results from the assumption of fixed surface air temperature toward which SST is restored. This restoring boundary condition keeps the SST anomalies small, thereby destabilizing the THC, as discussed by Zhang et al. In order to avoid this difficulty, *Rahmstorf and Willebrand* [1995] employed, for their ocean model, a scale-dependent upper boundary condition which permits SST anomalies of significant magnitude. This model was used effectively by *Rahmstorf* [1994, 1995] in his studies of the climatic response to the discharge of freshwater into the North Atlantic Ocean. His choice of a highly parameterized atmosphere, however, makes it very difficult to incorporate into this model other important interactions between the oceans and the atmosphere. Here we will attempt to overcome this difficulty by using a coupled model, in which an oceanic GCM is combined with a comprehensive atmospheric GCM.

2. Coupled Model

2.1. Model Structure

The coupled atmosphere-ocean-land surface model used in this study was developed for the study of the climate response to increasing greenhouse gases and will hereinafter be called the coupled model, for simplicity. The structure and performance of the model were described briefly by *Stouffer et al.* [1989] and in more detail by *Manabe et al.* [1991, 1992] and *Manabe and Stouffer* [1994]. The model consists of a general circulation model (GCM) of the global atmosphere coupled to a GCM of the oceans. Heat, water, and snow budgets at the continental surface are included. The model has global geography consistent with its computational resolution, and seasonal (but not diurnal) variation of insolation.

In the atmospheric component of the model, dynamic computations are performed using the so-called spectral element method [*Orszag*, 1970; *Gordon and Stern*, 1982], in which the distribution of a predicted variable is represented by a set of spherical harmonics (with 15 zonal waves and 15 associated Legendre functions) and values specified at grid points of 4.5° latitude and 7.5° longitude intervals. There are nine unevenly spaced levels for the finite differencing in the vertical direction. The effects of clouds, water vapor, carbon dioxide, and ozone are included in the calculation of both solar and terrestrial radiation. Water vapor and precipitation are predicted in the model [*Manabe et al.*, 1965], but a constant mixing ratio of carbon dioxide and a zonally uniform, seasonally varying vertical distribution of ozone are prescribed. Overcast cloud is assumed whenever relative humidity exceeds a critical value (99%). Otherwise, clear sky is predicted.

The ocean model of *Bryan and Lewis* [1979] has been modified as described by *Manabe et al.* [1991]. The finite difference mesh used for the time integration of the primitive equations of motion has a spacing between grid points of about 4.5° latitude and 3.7° longitude. It has 12 unevenly spaced levels in the vertical direction. In addition to the horizontal and vertical background subgrid-scale mixing and convective overturning, the model has isopycnal mixing as described by *Redi* [1982] and *Tziperman and Bryan* [1993]. The model predicts sea ice using a simple model that incorporates the thermodynamics and horizontal advection of sea ice by ocean currents [*Bryan*, 1969].

The atmospheric and oceanic components interact with each other through the exchanges of heat, water (including snow), and momentum at their interface. The water/snow flux includes runoff from the continents to the oceans. The runoff of snow from the continental ice sheets is determined from the budget of snow (on ice surface) which involves snowfall, sublimation, and snowmelt. We assumed here that the water-equivalent depth of snow does not exceed 10 cm and the underlying ice sheet does not melt, insuring that ice sheets remain essentially unchanged during the time integration of the coupled model. In the numerical experiments conducted here, freshwater is discharged, in addition, at oceanic surface as specified in section 3.

2.2. Time Integration

The initial conditions for the time integration of the coupled model have seasonal and geographical distributions of surface temperature, surface salinity, and sea ice of the present with which both the atmospheric and oceanic model states are nearly in equilibrium. When the time integration of the model starts from this initial condition, the model climate drifts toward its own equilibrium state, which differs from the initial condition described above. To reduce this drift, the fluxes of heat and water imposed at the oceanic surface (including sea ice-covered areas) of the coupled model are modified by amounts that vary geographically and seasonally but do not change from one year to the next (see *Manabe et al.* [1991] and *Manabe and Stouffer* [1994] for details). Since the adjustments are determined prior to the time integration of the coupled model and are not correlated to the transient anomalies of

SST and SSS (i.e., sea surface salinity), which can develop during its integration, they are unlikely to either systematically amplify or damp the anomalies. Owing to the flux adjustment technique described above, the model fluctuates around a realistic equilibrium state. One should also note, however, that this technique is quite different from the "restoring" that has been applied to SST and SSS during the time integration of an ocean-only model [e.g., *Bryan and Cox*, 1967], which strongly damps surface anomalies.

Starting from the initial condition that was obtained and described above, the coupled model is integrated over a period of 1000 years. Owing to the application of the flux adjustments, the mean trend in global mean surface air temperature during this period is very small and is -0.023°C century^{-1}. The trend of global mean temperature in the deeper layers of the model ocean is somewhat larger and is -0.07°C century^{-1}. This trend appears to result from the imperfection of the procedures which we developed for the determination of the initial condition and the time integration of the coupled model. The specific reasons for this trend, however, have not been identified and are under investigation.

3. Design of Freshwater Experiments

The simulated modern state of the coupled ocean-atmosphere system, which is obtained from the time integration described in section 2.2, is used as a control for the freshwater experiments conducted in the present study. Instead, one could have used as a control a coupled model state of the last deglaciation period when a major fraction of the continental ice sheets of the last glacial period still remained. Since the response of the cold, glacial state of the coupled ocean-atmosphere system could be different from the corresponding response of the interglacial, modern state [see, for example, *Winton*, 1996], it is highly desirable to conduct the numerical experiments with the boundary condition of the last deglaciation period. Unfortunately, we have not succeeded in simulating either the glacial or deglacial world using a coupled ocean-atmosphere GCM. This is why we use the simulated modern state of the coupled model as a control and perturbed it with an input of freshwater into the North Atlantic Ocean. It is encouraging, however, that a numerical experiment conducted earlier [*Manabe and Stouffer*, 1995] successfully simulated an abrupt climate change and was useful for elucidating the physical processes which control its evolution.

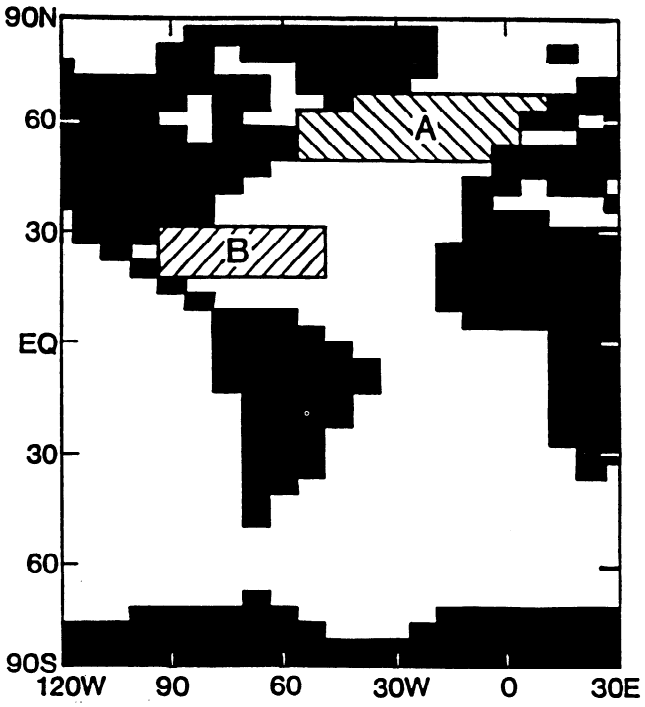

Figure 1. Regions A and B indicate the areas where freshwater is discharged in the first freshwater integration (FWN) and the second freshwater integration (FWS), respectively.

In addition to the control integration described in section 2.2, two numerical integrations are conducted for the present study. The initial condition for both integrations is the state of the coupled model at the 500th year of the control integration. In the first freshwater integration (FWN), the freshwater is discharged at the rate of 0.1 Sv (one sverdrup = 10^6 m^3 s^{-1}) uniformly over the 50°N-70°N belt of the North Atlantic Ocean (identified as domain A in Figure 1) over a period of 500 years. Although the freshwater input is terminated on the 500th year of the time integration, the FWN is continued for 750 more years until the 1250th year. By comparing the FWN with the control over a period of 1250 years, the impact of freshwater input upon the coupled ocean-atmosphere system is investigated.

In the second freshwater integration (FWS), freshwater is discharged uniformly over the subtropical region, identified as domain B (20.25°N-29.25°N, 52.5°W-90.0°W) in Figure 1, again at the rate of 0.1 Sv over a period of 500 years. This integration is completed at the 750th year (i.e., 250 years after the termination of the freshwater discharge).

In both numerical experiments, it is assumed that the temperature of discharged freshwater is identical to the local temperature of the mixed-layer ocean. Thus the freshwater input changes only surface salinity without affecting surface temperature.

4. Freshwater Experiment, North (FWN)

4.1. North Atlantic Ocean

In this section, we explore the response of the coupled ocean-atmosphere model in the FWN in which freshwater flux is infused into the 50°N-70°N belt of the North Atlantic Ocean over a period of 500 years. The time series of sea surface salinity (SSS), sea surface temperature (SST), and sea ice thickness are obtained at a grid point in Denmark Strait where the SST response is particularly large (Figure 2). Both SSS and SST decrease sharply during the first few hundred years of the FWN but more slowly during the remaining period of the water infusion. The slow-down is particularly notable with respect to the SST time series because of the formation and growth of sea ice (Figure 2c), which tends to anchor SST near the freezing point of seawater. As soon as the water infusion is terminated at the 500th year, SSS begins to rise very sharply and returns to its original value by the 750th year of the experiment. On the other hand, SST does not increase immediately

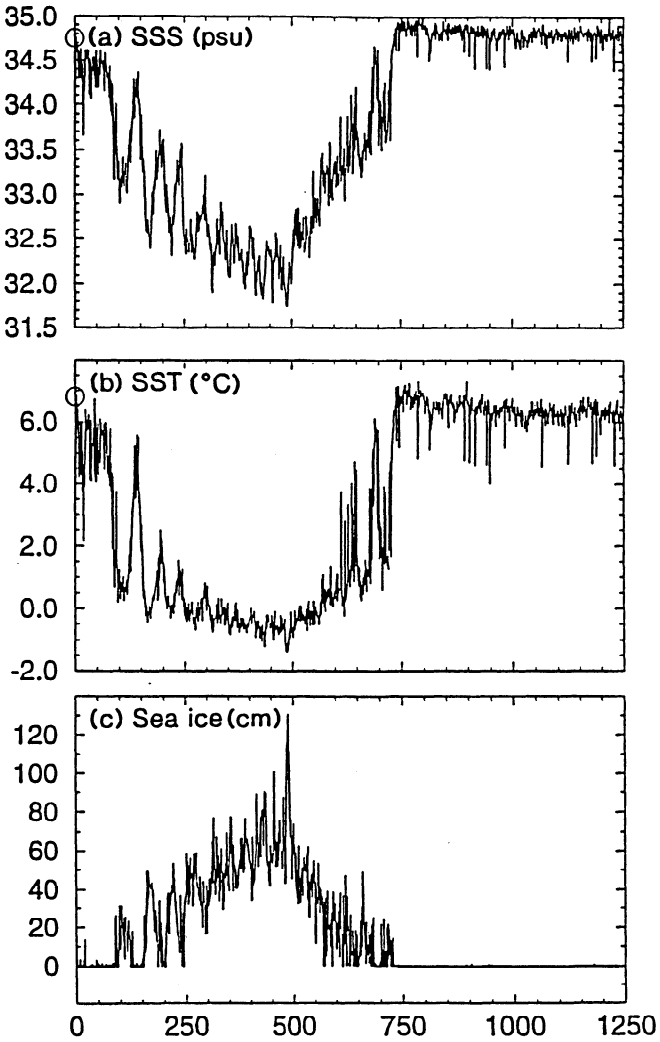

Figure 2. Time series of annual mean values of (a) sea surface salinity (SSS) (in practical salinity units (psu)), (b) sea surface temperature (SST) (°C), and (c) sea ice thickness (in centimeters) at a location (30.0°W, 65.3°N) in the Denmark Strait over the 1250-year period, obtained from the FWN. The initial values of SSS and SST are enclosed by circles.

after the termination of the water infusion, as it is constrained closely to the freezing point of seawater due to the melting of sea ice. As winter sea ice disappears about 100 years after the termination of the freshwater discharge, the rise of SST accelerates, returning to its original value around the 750th year of the experiment.

Superimposed upon the initial fall and eventual recovery of both SSS and SST described above, there exist rapid fluctuations of both variables on multidecadal timescales. Shortly after the start of the water discharge, very rapid drops of both SSS and SST occur, followed by large oscillations of both variables with a timescale ranging from several decades to a century. The amplitudes of oscillations gradually decrease until the termination of freshwater discharge (i.e., the 500th year) due to the growth of sea ice (Figure 2c), which reduces the anomalies of both SST and SSS through melting and freezing. The amplitude, however, increases again a few hundred years later, resulting in the very abrupt termination of the cold period. The large fluctuations in surface condition described above are associated with the fluctuation of the THC, as discussed later.

Despite the discharge of a large amount of freshwater over several centuries, the area of large SSS reduction is essentially confined to the region of the North Atlantic Ocean poleward of 40°N latitude and its Arctic extension (Figure 3). This suggests that the freshwater released in high latitudes of the North Atlantic Ocean hardly spreads toward the subtropical latitudes. SSS is reduced not only in the northern North Atlantic/Arctic regions but also in the zonally elongated patch in the Circumpolar Ocean of the southern hemisphere (Figure 3), as discussed briefly in the following subsection. In the rest of the world oceans, SSS increases very slightly.

The freshwater-induced cooling is particularly large over the northern North Atlantic and the Greenland/Iceland/Norwegian (GIN) Seas. It extends over not only Greenland but also the Arctic Ocean, the Scandinavian peninsula, and western Europe (Figure 4). One also notes that small negative anomalies extend over most of the high-latitude region of the northern hemisphere. The cooling centered around the GIN Seas increases until the end of the freshwater discharge (i.e., the 500th year of the experiment), but decreases rapidly thereafter and disappears completely by the 750th year. Negative SST anomalies also appear in the Indian and Pacific sectors of the Circumpolar Ocean in the southern hemisphere, extending to the Antarctic continent. On the other hand, very small positive SST anomalies cover the rest of the world. Because of the compensation between the extensive but small positive, and narrow but large negative anomalies described above, the global mean changes of surface air temperature turned out to be small during the experiment.

The distribution of the freshwater-induced change in surface air temperature described above is consistent with the map of the surface temperature difference between the Y-D and Alleröd, which was prepared by D. Peteet [*Broecker*, 1995] based upon the analysis of oceanic and bog sediments (Figure 5). The qualitative resemblance between the two patterns encourages the speculation that the cold climate of the Y-D could have resulted from the slow-down of the THC which was induced by the input of freshwater such as the discharge of the meltwater from the continental ice sheets. The pattern of the model-generated change, however, is placed somewhat to the north of the pattern of the Y-D/Alleröd difference as determined from proxy data. As discussed in section 6, this difference may partly be attributable to the fact that the freshwater flux is applied to the simulated, modern state of the coupled ocean-atmosphere model which is much warmer than the cold state of the deglacial period. Thus the albedo feedback process involving sea ice and snow operates at higher latitudes than it should, placing the pattern of freshwater-induced temperature change poleward of the regions of the Y-D cooling.

The input of freshwater also induces a large variation of the THC in the Atlantic Ocean as indicated in Figure 6a. Originally, the THC in the North Atlantic Ocean has the intensity of ~18.5 Sv. It weakens very rapidly during the first 50 years of freshwater input, but at a somewhat slower rate during the

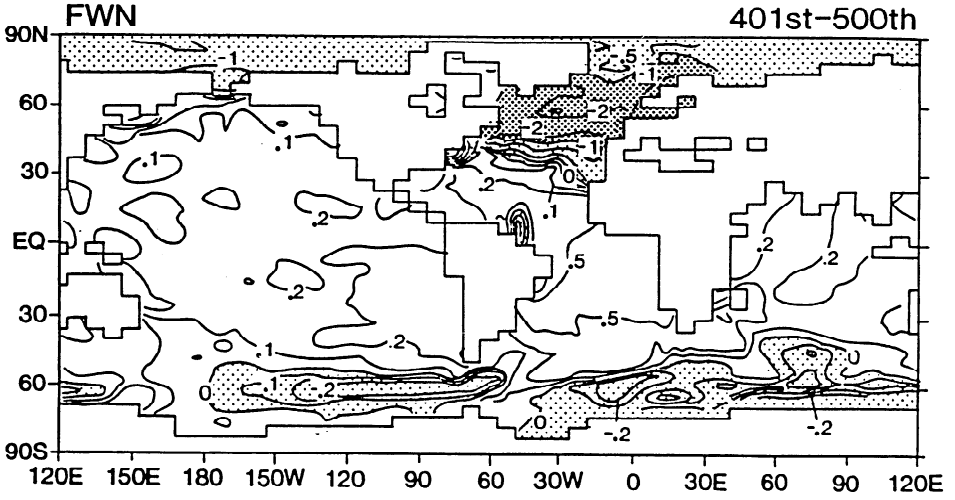

Figure 3. The geographical distribution of SSS anomalies (psu) averaged over the 401st-500th year of the FWN. Here anomaly represents the difference between the FWN and the control experiment. Contours are drawn in logarithmic intervals for values of 0, ±0.1, ±0.2, ±0.5, ±1, and ±2.

next few hundred years until it is reduced down to the intensity of about 3.5 Sv at the end of the freshwater infusion period (i.e., the 500th year). However, upon the termination of the freshwater discharge, the THC begins to intensify rapidly, slightly exceeding the original intensity by the 750th year of the experiment.

The temporal variation in the intensity of the THC in the North Atlantic Ocean (Figure 6a) resembles the variation of the surface water density at a location in the Denmark Strait shown in Figure 6b. One also notes that the time series of surface water density in Figure 6b resembles that of SSS shown in Figure 2a, indicating the dominating influence of SSS upon the density of surface water in high latitudes where SST is close to the freezing point. As SSS is reduced in the northern North Atlantic Ocean during the 500-year period of the freshwater discharge, the surface water density is also reduced (Figure 6b), thereby reducing the vertical convective mixing in the ocean (Figure 6c) and the heat loss from the oceanic

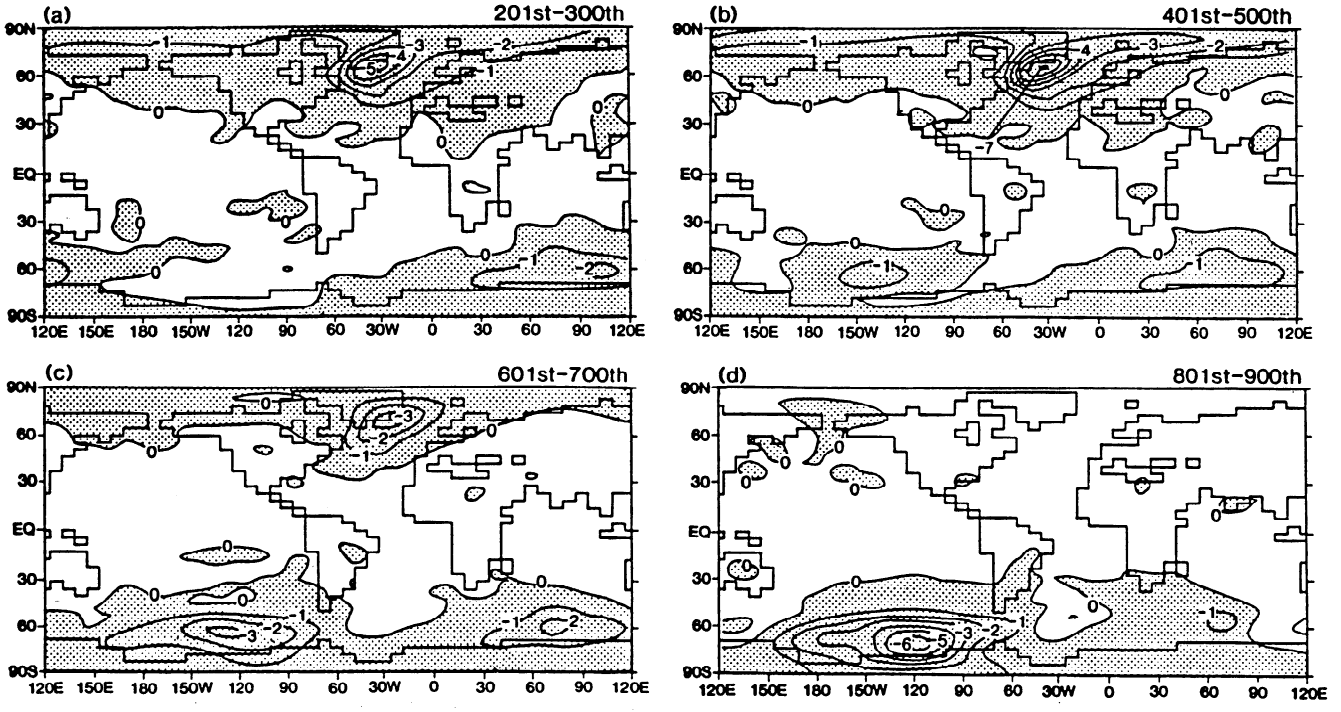

Figure 4. The geographical distributions of surface air temperature anomalies (°C) averaged over (a) the 201st-300th year, (b) the 401st-500th year, (c) the 501st-600th year, and (d) the 801st-900th year, of the FWN. Here anomaly represents the difference between the FWN and the control experiment.

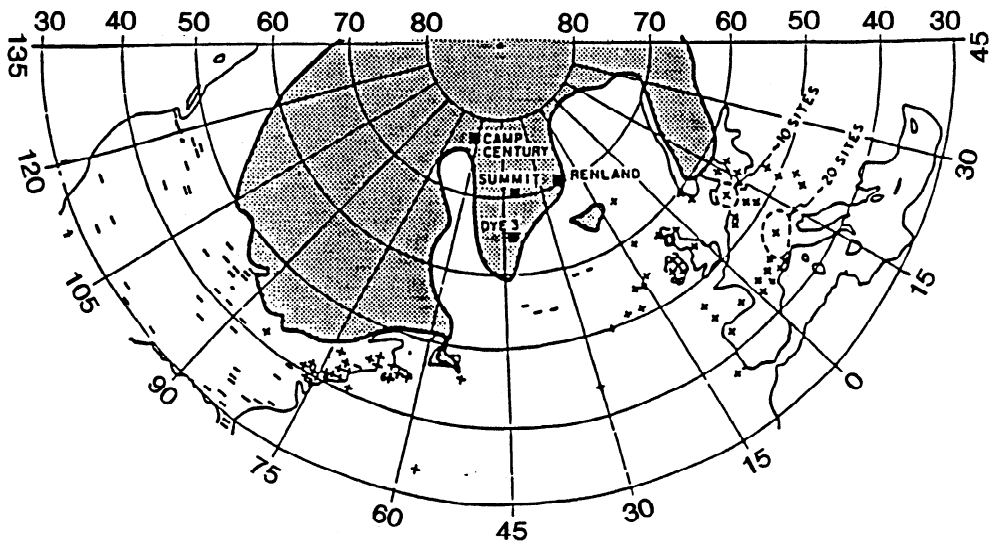

Figure 5. Map prepared by D. Peteet showing sites of ocean sediment (planktonic forams) and bog sediments (pollen grains) where records covering the interval of deglaciation are available. The pluses indicate that the Younger-Dryas event (Y-D) cooling is seen, and the minuses indicate that it is not. Two pluses are added by the present authors at 43.5°N, 29.9°W and 33.7°N, 57.6°W, referring to the studies of *Keigwin and Lehman* [1994], and *Keigwin and Jones* [1989], respectively. The location of the Greenland ice cores (all show the Y-D) are also given. The shaded region shows the area coverage of the ice cap at the time of the Y-D [from *Broecker*, 1995]. See also Figure 6 of *Peteet* [1995], which indicates the global distribution of polynological evidence for the Y-D cooling.

surface to the overlying atmosphere. The reduction of the heat loss, in turn, makes it more difficult for water to sink, thereby weakening the THC. The slow-down of the THC reduces the northward advection of saline water, contributing to further reduction of SSS. The weakening of convective activity and the reduction of the northward advection of warm surface water in the northern North Atlantic also contribute to the continued reduction of SST throughout the 500-year period of the water discharge (Figure 2b).

In high North Atlantic latitudes of the coupled model, deep convection takes place mainly in three regions, namely to the southeast of Greenland, near the Labrador Sea, and near Spitzbergen. Convective activity in these regions varies on all timescales ranging from days to centuries or longer. In response to the freshwater discharge, both convective activity and the THC weaken greatly in the FWN experiment.

As the water discharge is terminated at the 500th year of the FWN experiment, SSS starts increasing rapidly in the northern North Atlantic Ocean (Figure 2a) because of the advection and diffusion of the relatively fresh surface water away from the region of discharge. Thus the density of the surface layer increases (Figure 6b), enhancing the convective activity there. As the convective mixing of seawater increases in the sinking regions of the THC, the THC rapidly intensifies, recovering its original intensity only a few hundred years after the termination of water discharge.

The stream function of the meridional overturning in the Atlantic Ocean (Figure 7) indicates that the THC not only weakens but also becomes much shallower by the end of the 500-year infusion of freshwater. Meanwhile, the northward flow of the Antarctic bottom water extends northward, thereby intensifying the counterclockwise overturning cell near the bottom of the Atlantic Ocean (Figure 7b). Following the termination of freshwater discharge, the THC rapidly reintensifies and recovers the original intensity and distribution by the 1000th year of the experiment (Figure 7c).

As the intensity of the THC weakens, the surface currents in the North Atlantic Ocean also undergo marked changes, which can be inferred by comparing Figures 8a and 8b. For example, the North Atlantic Current, which extends from the Florida coast to the Norwegian Sea, also weakens in the Atlantic throughout the period of the water infusion. Thus the warm, saline surface water in the subtropical Atlantic hardly penetrates into the northern North Atlantic Ocean toward the end of the 500-year discharge of freshwater. It is of particular interest that the intensified Labrador current and its southeastward extension track the path of ice-rafted debris [*Bond et al.*, 1992] during the cold period of the Dansgaad-Oeschger Oscillations, which appear to resemble the Y-D event in many respects.

Superimposed upon the weakening and intensification of the THC over several centuries, one notes the multidecadal fluctuation of the THC which follows the sudden onset of the freshwater discharge at the beginning of the experiment (Figure 7a). The timescale and the structure of the fluctuation resembles the internally generated, multidecadal oscillation which *Delworth et al.* [1993, 1997] found in a long-term integration of the coupled ocean-atmosphere model without a freshwater forcing. However, its amplitude is much larger than that of Delworth et al. The multidecadal fluctuation of the THC is in phase with the corresponding fluctuations of SSS and SST which were described already (Figures 2a and 2b). As the intensity of the THC changes, both SSS and SST change almost concurrently. The change in salinity, in turn,

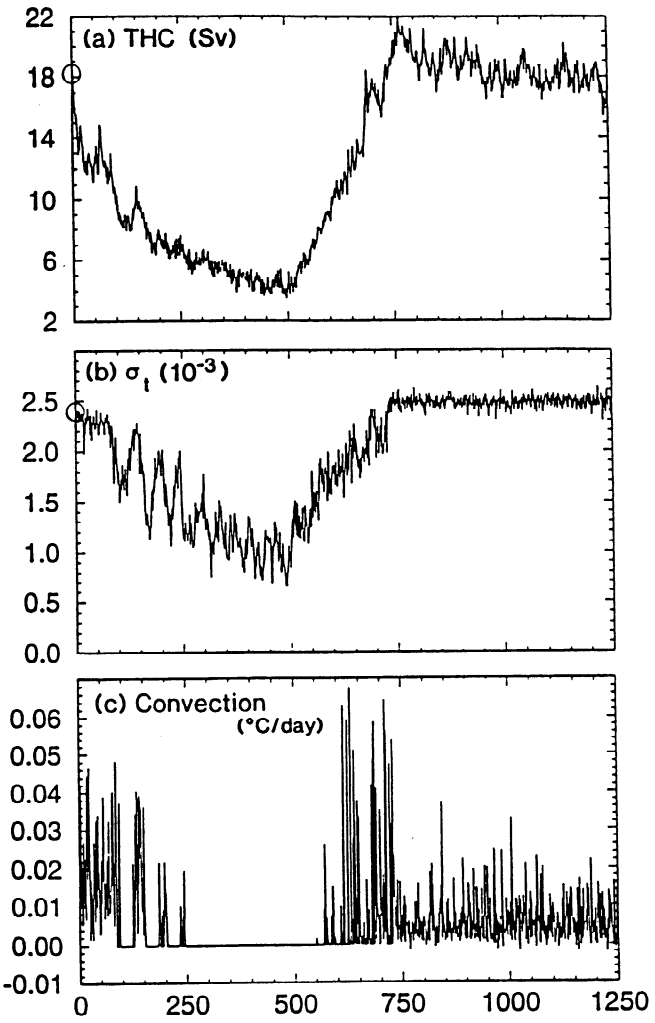

Figure 6. Time series of annual mean values of (a) the intensity of the thermohaline circulation (THC) (one sverdrup = 10^6 m^3 s^{-1}) in the North Atlantic Ocean (defined as the maximum value of stream function of the THC), (b) the density of surface water as represented by σ_t in units of parts per thousand, and (c) the rate of surface temperature change (°C d^{-1}) due to convective adjustment in model oceans at a location (30.0°W, 65.3°N) in the Denmark Strait over the 1250-year period, obtained from the FWN. The initial values of the THC intensity and σ_t are enclosed by circles.

dominates the changes in the density of the near-surface layer around the sinking regions of the THC (Figure 6b). It appears that the variation of surface water density alters not only the convective activities but also the downward velocity in the sinking region, enhancing further the fluctuation of the THC.

The temporal variation of SST discussed earlier affects the temperature of the overlying air, as indicated in Figure 9a. In response to the freshwater input, the surface air temperature in Denmark Strait falls and rises with a timescale of ~800 years in a manner quantitatively similar to the evolution of the THC in the North Atlantic Ocean. The surface air temperature at a grid point close to Summit, Greenland (Figure 9b), also undergoes a similar but smaller fluctuation. The drop and recovery of surface air temperature at the beginning and after the termination of the water discharge appear to be more gradual than the very rapid changes of isotopic temperature at the beginning and the end of the Y-D. Upon close inspection of the

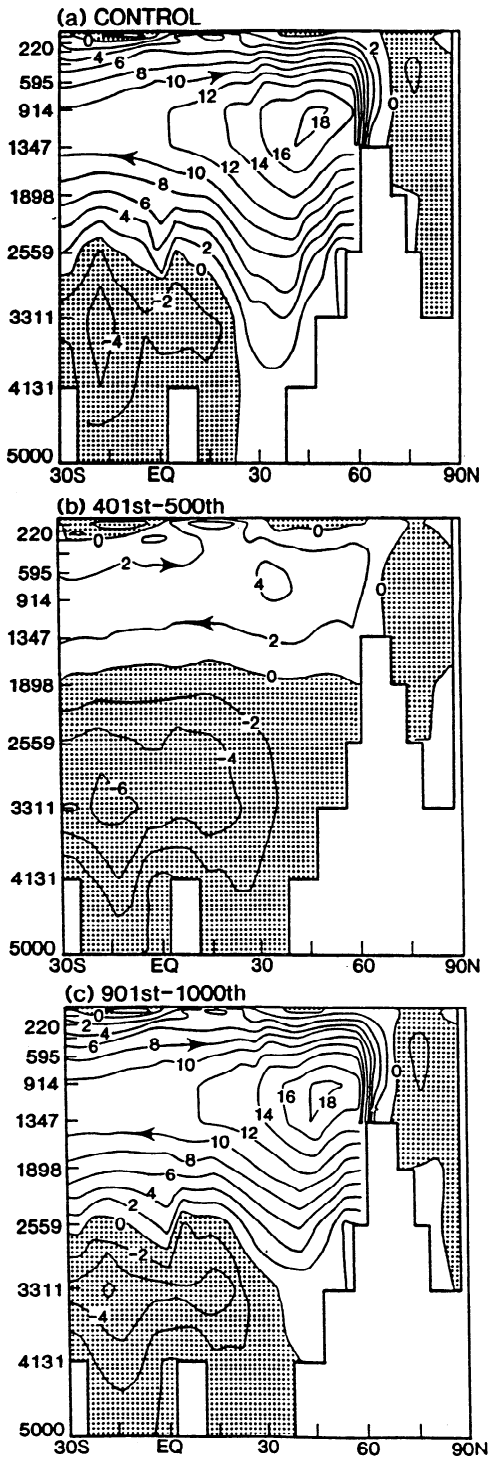

Figure 7. Stream function of the THC in the Atlantic Ocean of the coupled model in units of sverdrups. (a) Control experiment (100-year average taken just before it branches off to the FWN). (b) Average over the 401st-500th year of the FWN. (c) Average over the 901st-1000th year of the FWN. On the left-hand side of each panel, depth is indicated in meters.

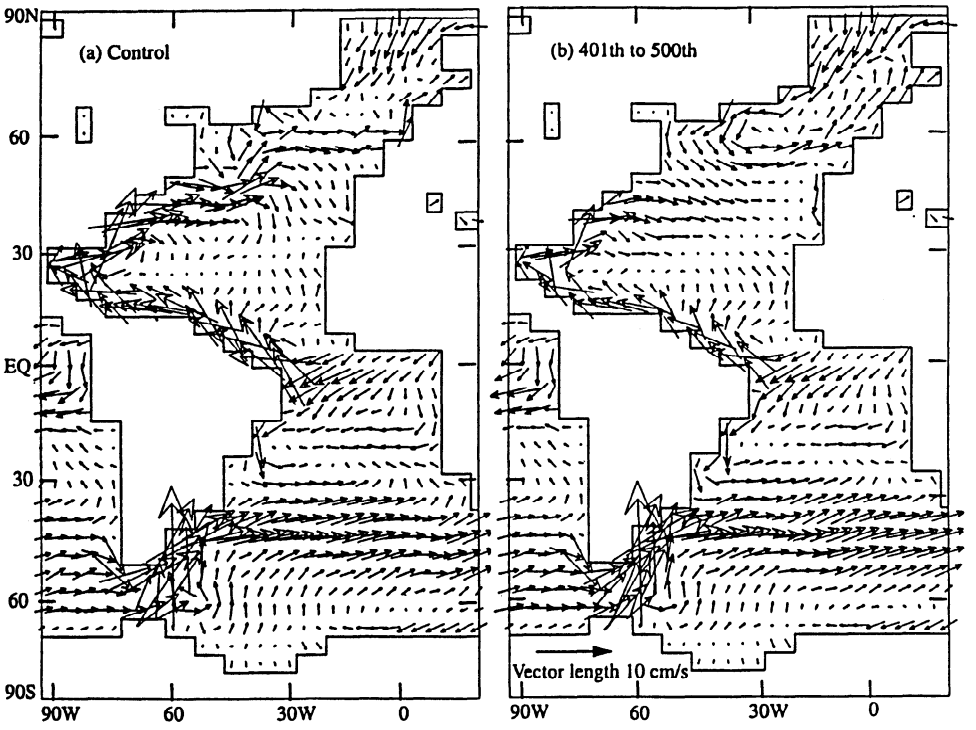

Figure 8. Map of surface current vectors. (a) Control experiment (100-year average taken just before branching off to the FWN). (b) Average over the 401st-500th year of the FWN.

Summit time series in Figure 9b, one notes, however, the large and rapid fall of surface air temperature between the 70th and the 110th year and the rapid rise between the 660th and the 760th year of the experiment. The large multidecadal fluctuations of SST, associated with the oscillation of the THC, are superposed upon the multicentury variation of SST, yielding the large and rapid changes of surface air temperature described above. The numerical experiment conducted earlier by *Manabe and Stouffer* [1995] indicates that a larger rate of freshwater discharge at the beginning of the present experiment could have yielded an even more abrupt drop of surface temperature.

The model atmosphere is not a passive participant in the simulated cooling event. Associated with the cooling, positive sea level pressure anomaly (max. ~4mb) with meridionally elongated pattern develops around the southeastern Greenland, resulting in the weakening and eastward shift of the Icelandic Low and the marked weakening of southerly wind in the GIN Seas. Thus, the East Greenland Current intensifies, enhancing the reduction of SST around the Denmark Strait. The weakening of the Icelandic Low also leads to a reduction in the westerlies and equatorward Ekman drift current which could contribute to the reintensification of the THC (see, for example, *Weaver et al.* [1993] for the discussion of this wind stress feedback process). The change of surface wind associated with the sea level pressure anomaly described above alters the advection of surface temperature, resulting in the change of SAT in the regions which surround the GIN Seas (see Figure 4).

4.2. Circumpolar Ocean

In response to the freshwater input, the surface cooling occurs not only in the North Atlantic Ocean but also in the Circumpolar Ocean of the southern hemisphere (Figure 4). For example, the negative anomaly of surface air temperature increases until the termination of the water discharge (i.e., the 500th year of the experiment) and weakens thereafter in the Atlantic/Indian Ocean sector of the Circumpolar Ocean. In the Pacific sector, the negative anomaly continues to grow until the 800th year of the experiment, extending to the interior of the Antarctic continent. Because of the albedo feedback effect of sea ice, the cold anomaly could have extended northward if the freshwater were applied to the cold state of the deglacial period rather than the warm modern state obtained from the control experiment. It is therefore likely that major advances of mountain glaciers in the New Zealand Alps [e.g., *Denton and Hendy*, 1994; *Basher and McSaveney*, 1989] during the Y-D could be caused by the cooling of the Circumpolar Ocean. With regard to the cooling over the Antarctic continent, it is worthwhile to determine whether the cold reversal of surface temperature in the Pacific sector of the Antarctic continent [e.g., *Mayewski et al.*, 1996] lags behind that of the Atlantic/Indian Ocean sector [e.g., *Jouzel et al.*, 1995] as simulated by the model.

The development of the negative surface temperature anomalies in the Circumpolar Ocean of the southern hemisphere appears to result from not only the changes of the THC in the Atlantic Ocean but also the associated change of the re-

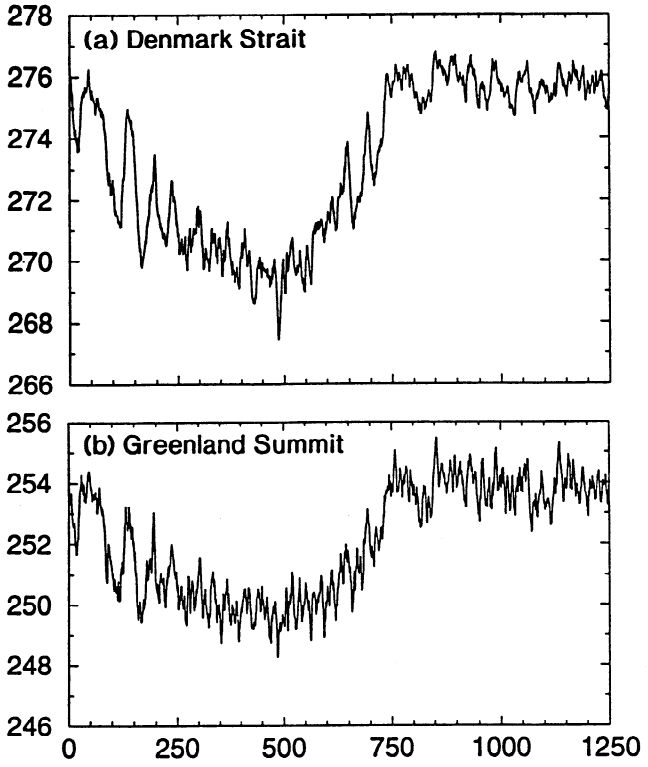

Figure 9. Time series of 5-year running mean surface air temperature (in Kelvins) (a) at a location (30.0°W, 65.3°N) in the Denmark Strait and (b) at a grid point (37.5°W, 74.25°N) near Summit, Greenland, over the 1250-year period, obtained from the FWN. The initial values are enclosed by circles.

verse circulation cell in the deep Pacific Ocean (Figure 10). Although the THC in the North Atlantic Ocean stops weakening when the water discharge is terminated at the 500th year of the experiment (Figure 6a), the reverse circulation in the Pacific Ocean continues to weaken until approximately the 950th year (Figure 11). The weakening of the overturning circulation described above raises the temperature in the upper layers of both the Atlantic and Pacific Oceans in low to middle latitudes (Figure 12). In the Atlantic Ocean, the positive subsurface temperature anomaly becomes more pronounced until the termination of the freshwater input at the 500th year but weakens rapidly as the THC reintensifies. In the Pacific Ocean, the positive anomaly in the upper oceanic layer keeps growing until the 950th year or so. Gradually extending to the surface of both oceans, the warm anomalies in the southern hemisphere increase the meridional gradients of both SST and lower tropospheric temperature to their south, intensifying the westerlies in the atmosphere (Figure 13). The intensification of surface westerlies, in turn, accelerates the northward Ekman drift of surface water and sea ice, extends the sea ice coverage northward, and reduces the temperatures of the mixed-layer ocean (Figure 12b) and overlying air, particularly near the southern margin of the Ekman drift belt, further increasing the meridional gradient of the lower tropospheric temperature (Figure 13b). The mutually enhancing relationship between the Ekman drift and the westerlies contributes to the slight reduction of surface air temperature in the Atlantic sector, followed by the major reduction in the Pacific sector of the Circumpolar Ocean of the southern hemisphere. The increased Ekman drift of surface water reduces not only SST but also SSS in the Circumpolar Ocean (Figure 3).

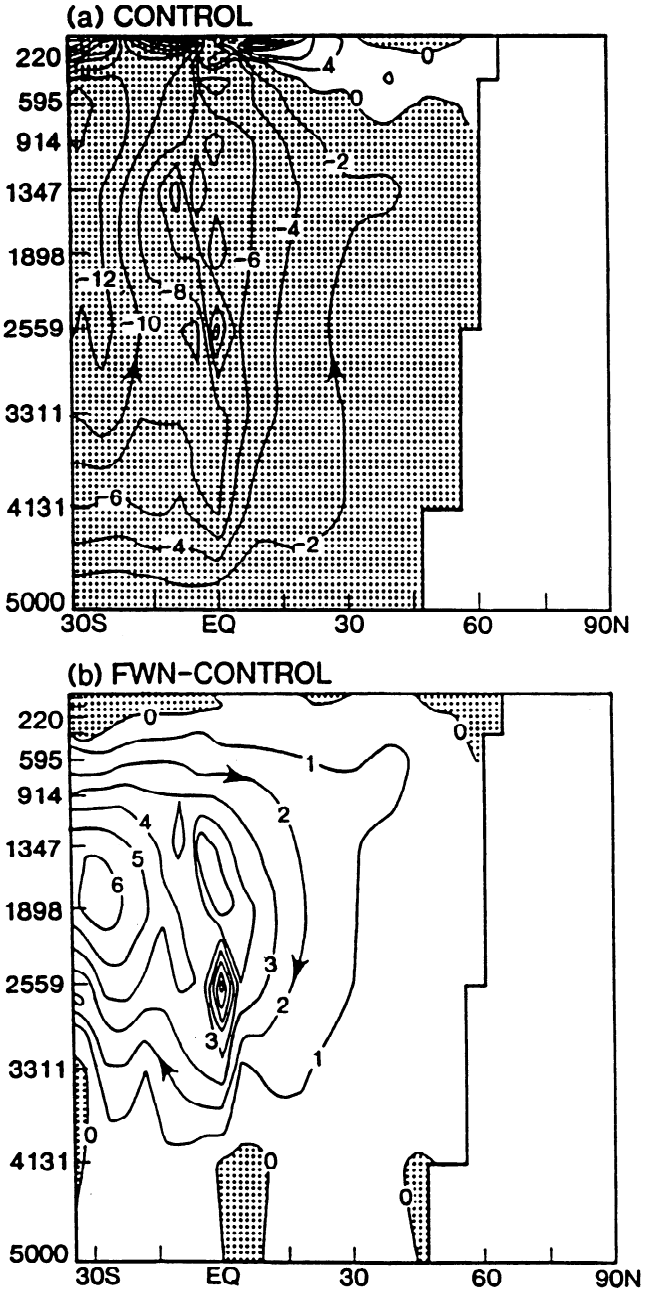

Figure 10. Stream function of meridional overturning in the Indo-Pacific Ocean in units of sverdrups. (a) Control experiment (100-year average taken just before it branches off to the FWN). (b) Difference between the FWN and the control averaged over the 401st-500th year of the FWN. On the left-hand side of each panel, depth is indicated in meters.

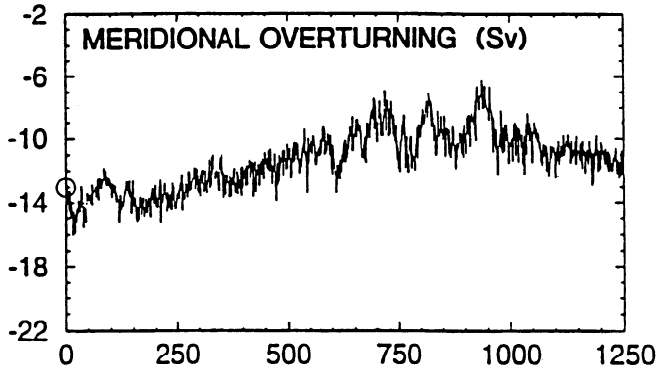

Figure 11. Time series of the largest negative value of annual mean stream function of the meridional overturning in the Indo-Pacific Ocean over the 1250-year period, obtained from the FWN. Units are in sverdrups.

5. Freshwater Experiment, South (FWS)

In this section, we evaluate the impact of the subtropical discharge of freshwater upon the coupled model in comparison to the high-latitude discharge experiment (i.e., FWN) described in the preceding section. As noted earlier, the magnitude and duration of the subtropical freshwater discharge are chosen to be identical to those of the high-latitude discharge for the ease of comparison. However, the negative SSS anomalies in the North Atlantic Ocean are much smaller in the FWS than in the FWN throughout the course of the experiments (compare Figure 14 with Figure 3). Because of the difference in the magnitude of the negative SSS anomalies in the sinking region of the THC, the total reduction of the THC intensity during the period of the freshwater discharge is smaller in the FWS by a factor of ~5 than in the FWN (compare Figures 15 and 6a). As a matter of fact, the THC in the FWS stops weakening a few hundred years before the termination of the freshwater discharge in the 500th year of the experiment (Figure 15). In sharp contrast to the FWN in which the THC weakens markedly and negative SSS anomalies are enhanced due to the reduction in the northward advection of relatively saline surface water, the freshwater-induced SSS anomalies in the FWS are reduced by oceanic circulation and remain small in the North Atlantic Ocean.

In order to compare the freshwater-induced changes of the coupled systems obtained from the two experiments, the horizontal distributions of the SST anomalies from both FWN and FWS are shown in Figure 16. Again, the magnitude of negative SST anomalies in the FWS is much less than the FWN. It is notable, however, that the two distributions of the SST anomalies resemble each other, with relatively large negative anomalies in the northern North Atlantic, the Circumpolar Ocean of the southern hemisphere, and the northwestern region of the Pacific Ocean. The distributions of the thermal responses of the coupled model are similar not only at the surface but also in the subsurface layer of the model oceans, underscoring the similarity of the dynamical mechanism involved.

In short, the subtropical discharge of freshwater is much less effective in weakening the THC and altering the thermal structure of the oceans as compared with the high-latitude discharge in the FWN. In assessing the impact of a meltwater discharge upon a so-called abrupt climate change such as the Y-D event, it is therefore very important to reliably determine the location of meltwater discharge.

6. Concluding Remarks

In response to the discharge of freshwater into a high-latitude belt of the North Atlantic Ocean, the THC of a coupled ocean-atmosphere model weakens, reducing surface air temperature over the northern North Atlantic, the GIN Seas, and Greenland, and to a lesser degree, over the Arctic Ocean, the Scandinavian peninsula, Labrador, and the Circumpolar Ocean of the southern hemisphere. Upon the termination of the water discharge in the 500th year of the experiment, the THC begins to intensify rapidly, regaining its original intensity in a few hundred years. With the exception of the Pacific sector of the Circumpolar Ocean where surface air temperature continues to decrease beyond the 500th year, the climates of the northern North Atlantic and surrounding regions also recover rapidly.

The evolution of the ocean-atmosphere system described above resembles the Y-D event as inferred from the comprehensive analysis of ice cores and deep-sea and lake sediments [see, for example, *Broecker*, 1995]. However, the patterns of cooling in both the North Atlantic and Circumpolar Oceans appear to be placed poleward of the Y-D cooling. The simulated cooling at Summit, Greenland, appears to be smaller than the actual cooling as estimated from the isotopic analysis of ice cores [e.g., *GRIP Members*, 1993]. Although the cooling also occurs in the Circumpolar Ocean of the southern hemisphere, it does not extend northward sufficiently to induce the major advance of glaciers in New Zealand mentioned earlier. We speculate that these discrepancies result partly from the use of the simulated modern climate as a control rather than the much colder climate of the last deglaciation period. The extensive coverage of sea ice during the cold deglaciation period could not only have extended the regions of cooling toward lower latitudes but could also have increased its magnitude. It is therefore desirable to conduct additional freshwater experiments using the simulated climate of the last deglaciation period as a control.

Improving the earlier results of *Guilderson et al.* [1994], *Guilderson* [1996] obtained the high-resolution time series of SST based upon the Sr/Ca thermometry of Barbados corals. His time series indicates that the surface temperature of the western tropical Atlantic fell rapidly during the late Bölling period (between 15 and 13.8 Kyr B.P.), when the massive discharge of freshwater (identified as mwp-IA by *Fairbanks* [1989] took place. Upon the termination of the mwp-IA (i.e., around 13.7 Kyr B.P.), it rises rapidly. It is notable, however, that the Sr/Ca temperature did not change substantially at the beginning of the Y-D (i.e., around 13 Kyr B.P.), despite the abrupt drop of surface temperature in high Atlantic latitudes.

These findings are not inconsistent with the result of the present FWN experiment in which SST in tropical latitudes hardly changes (Figure 16) despite the large meltwater-induced change in the intensity of the THC. On the other hand, the rapid fall of Sr/Ca temperature in the western tropical Atlantic during the late Bölling (between 15 and 13.8 Kyr B.P.)

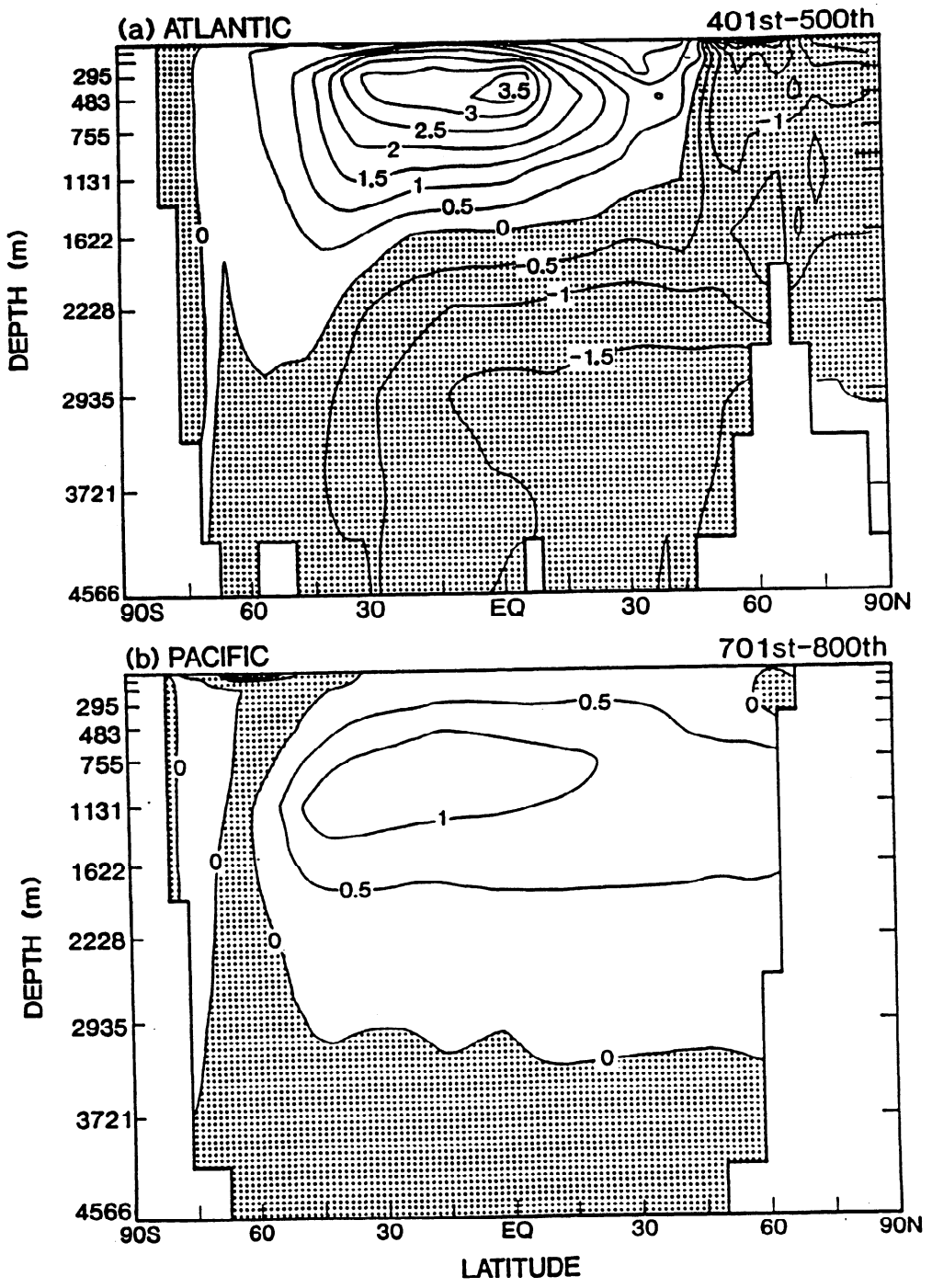

Figure 12. (a) Zonal mean temperature anomaly (°C) in the Atlantic Ocean averaged over the 401st-500th year. (b) Zonal mean temperature anomaly (°C) in the Indo-Pacific Ocean averaged over the 701st-800th year. Here anomaly represents the difference between the FWN and the control experiment. On the left-hand side of each panel, depth is indicated in meters.

could result from the cooling of the mixed-layer ocean caused by the massive discharge of cold freshwater into the Gulf of Mexico, as suggested by *Guilderson* [1996].

One should note, however, that *Thompson et al.* [1995] found evidence of the Y-D cooling in the tropical atmosphere based upon the isotopic analysis of two ice cores obtained from the col of Huascarán (9° 06′ S, 77° 36′ W). In view of the absence of tropical cooling in the present experiments, it is likely that the cooling of the tropics during the Y-D was not caused by the weakening of the THC which was induced by the discharge of freshwater. Instead, it may have been caused by other factors such as the reduction in the atmospheric con-

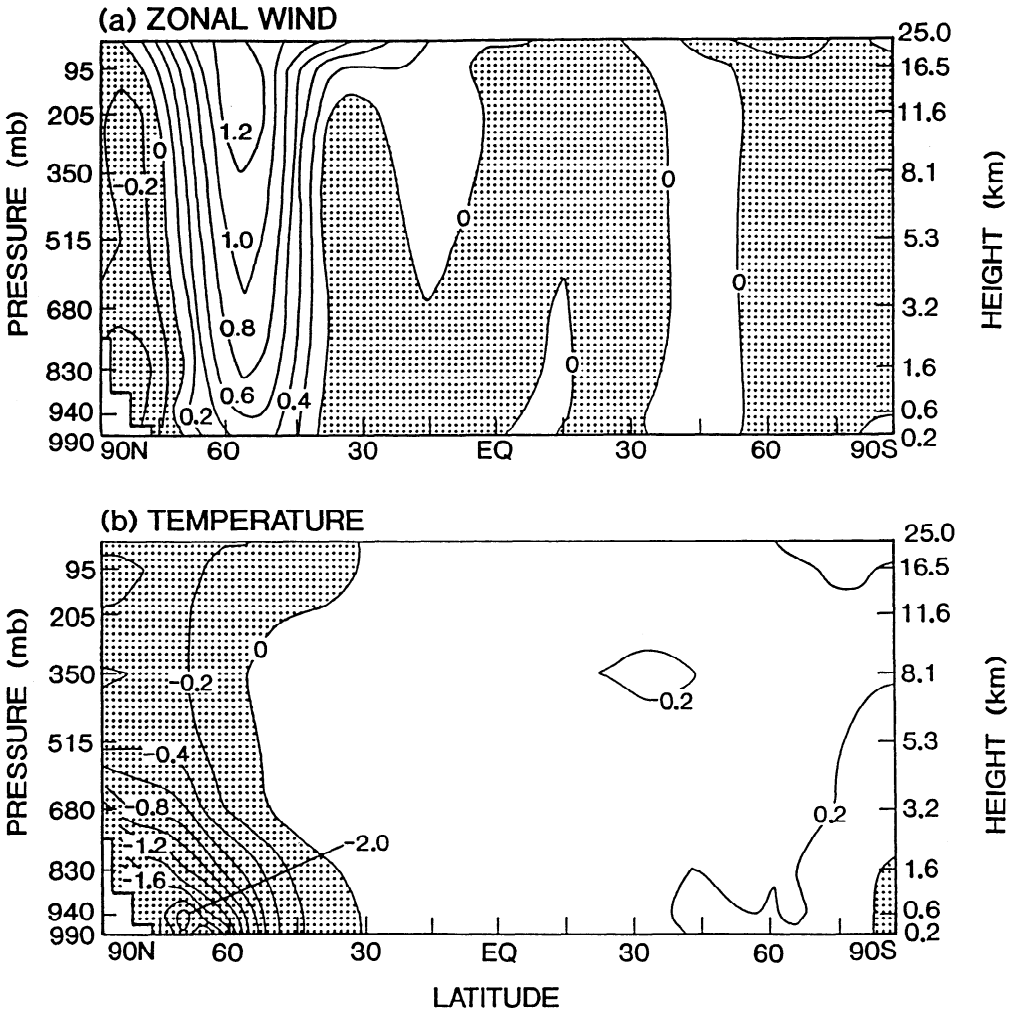

Figure 13. Latitude-height distributions of (a) annually averaged zonal mean wind anomaly (in meters per second) and (b) annually averaged zonal mean temperature anomaly (°C) in the 701st-800th year of the FWN. Here anomaly is defined as the difference between the FWN and control experiment. Pressure (in millibars) and approximate height (in kilometers) are indicated on the left- and right-hand sides of each panel, respectively.

centration of methane in the atmosphere [*Chappellaz et al.*, 1993].

Two numerical experiments are conducted in the present study. In the first experiment discussed above (FWN), freshwater is discharged into the high North Atlantic latitudes which include the sinking regions of the THC, whereas it is applied to a region of the subtropical Atlantic in the second experiment (FWS). In the FWN, the THC weakens because of the capping of the sinking regions by relatively fresh, low-density surface water. On the other hand, the negative SSS anomaly over the sinking regions is much smaller and is much less effective for weakening the THC in the FWS in which freshwater is discharged in the subtropical Atlantic.

The contrast between the results from these two experiments encourages the speculation that the diversion of meltwater from the Mississippi to the St. Lawrence [*Hansel and Michelson*, 1988] helped to weaken the THC, inducing the cold climate of the Y-D, as suggested by *Broecker et al.* [1988]. One can also speculate that the northward transport of heat by the active THC during the warm period of Alleröd could have induced the accelerated melting of the Eurasian Ice Sheets, which in turn slows down the THC in the Atlantic Ocean. This speculation appears to be consistent with the high-resolution records of oxygen isotope and the diatom summer SST from a Norwegian Sea core [*Karpuz and Jansen*, 1992]. Despite the rapid drop of the diatom temperature from the Alleröd to Y-D, the oxygen isotope anomaly (adjusted for global ice volume) decreases steadily with time, suggesting the possible discharge of meltwater from the Fennoscandian Ice sheets prior to and at the beginning of the Y-D.

As noted already, the coral records of sea level indicate that the mwp-IA ended several hundred years before the onset of the Y-D [*Guilderson*, 1996; *Bard et al.*, 1996]. *Keigwin et al.* [1991] and *Fairbanks et al.* [1992] traced a possible origin of this meltwater discharge back to the Gulf of Mexico. The comparison between the FWN and FWS experiments sug-

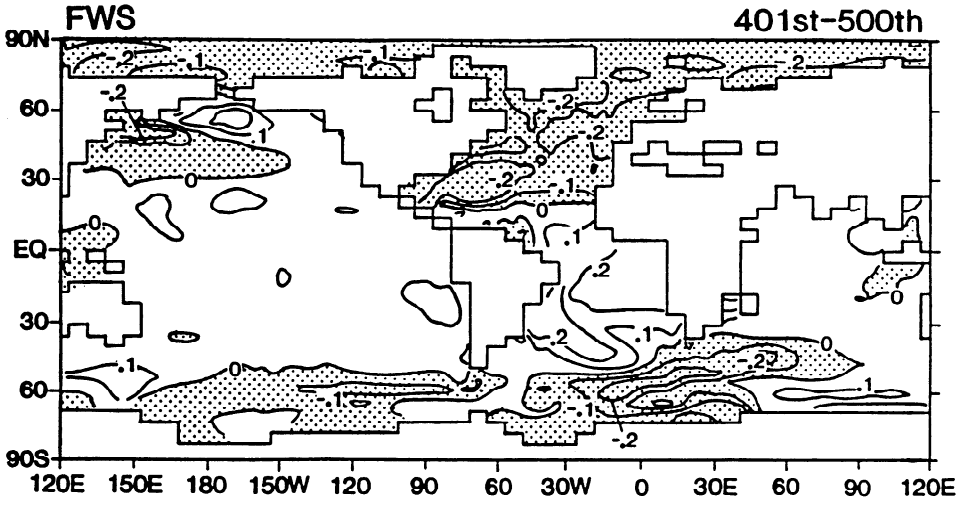

Figure 14. Horizontal distribution of SSS anomaly (psu) averaged over the 401st-500th year of the FWS. Here anomaly is defined as the difference between the FWS and the control experiment.

gests that the subtropical discharge of meltwater such as the mwp-IA may be much less effective than the high-latitude discharge in weakening the THC. However, the massive amount of freshwater involved in the mwp-IA could be sufficient to weaken the THC significantly and induce the cooling of the late Bölling (between 15 and 13.8 Kyr B.P.).

On the other hand, *Clark et al.* [1996] suggested that the Mississippi River may not be the primary source of water for the mwp-IA. Their ice sheet models suggest that the southern sector of the Laurentide Ice Sheet could contribute only a fraction (<10%) of sea level rise associated with the mwp-IA, leaving the Antarctic Ice Sheet as the only other ice sheet capable of delivering enough water to account for mwp-IA. If their estimate were correct, the meltwater from the Mississippi River Basin would be far from sufficient to induce the substantial weakening of the THC.

As discussed in section 4.2, the simulated cooling in high southern latitudes lags behind the cooling in the North Atlantic by several centuries. If the response of the model were realistic, it is not very likely that the rapid Y-D cooling which occurred around 13 Kyr B.P. induced a small drop of isotopic temperature near the Byrd Station of Antarctica which occurred between 12.5 and 14 Kyr B.P. [*Sowers and Bender*, 1995]. Instead, one can speculate that the North Atlantic cooling of the late Bölling period discussed above could have induced the drop of Byrd isotopic temperature between 12.5 and 14 Kyr B.P.

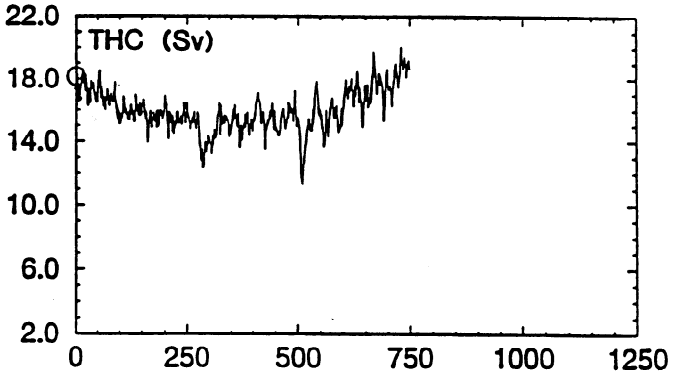

Figure 15. Time series of the intensity of the THC in the Atlantic Ocean over the period of 750 years, obtained from the FWN. The initial value is enclosed by a circle. Here the intensity is defined as the maximum value of the stream function representing the meridional overturning circulation. Units are in sverdrups.

Manabe and Stouffer [1988] found that their coupled ocean-atmosphere model has at least two stable equilibria with active and inactive modes of the THC in the Atlantic Ocean. The active mode resembles the current state of the North Atlantic, whereas the inactive mode is characterized by the weak, reverse cell of the THC but also by the very thick, upper ocean layer of low salinity which extends all the way to low latitudes of the North Atlantic Ocean. They suggested that an oceanic state similar to this inactive mode prevailed during the period of the Y-D. Paleoceanographic evidences, however, do not necessarily support this suggestion. Although the deep-sea cores from the North Atlantic Ocean indicate markedly reduced deep water formation [*Boyle and Keigwin*, 1987; *Keigwin and Lehman*, 1994], the distribution of benthic $\delta^{13}C$ determined by *Sarnthein et al.* [1994] suggests that the upper deep water production of significant magnitude did occur during the Y-D. Paleoceanographic evidences [*Boyle and Keigwin*, 1987; *Duplessy et al.*, 1988] indicate that the Atlantic Ocean of the last glacial maximum (LGM) is also significantly different from the inactive mode of the THC obtained by *Manabe and Stouffer* [1988]. It is characterized by not only the absence of lower deep water production and enhanced northward penetration of the Antarctic bottom water, but also significant ventilation of the upper deep water. Thus it is likely that the North Atlantic Ocean of the Y-D or the LGM are more similar to the transient state of the weakened and shallow THC (obtained from the present experiment) than the equilibrium state of the inactive THC obtained earlier by *Manabe and Stouffer* [1988].

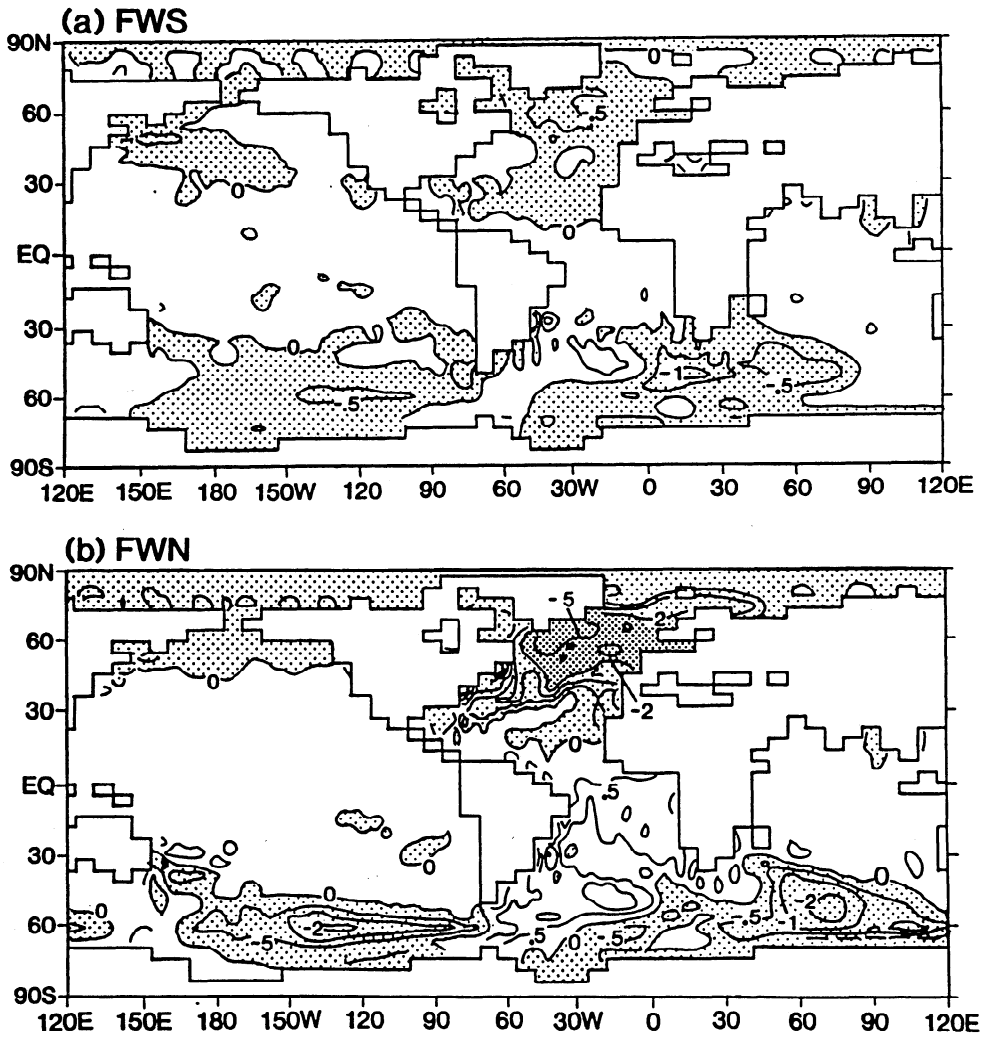

Figure 16. Time series of the intensity of the THC in the Atlantic Ocean over the period of 750 years, obtained from the FWN. The initial value is enclosed by a circle. Here the intensity is defined as the maximum value of the stream function representing the meridional overturning circulation. Units are in sverdrups.

The coupled model used here also possesses the two stable equilibria which are similar to those obtained by *Manabe and Stouffer* [1988]. When it is induced, the state of the inactive THC is stable and remains unchanged over the period of at least several thousand years. Despite the heating due to the vertical thermal diffusion, the temperature of the bottom water does not increase because of the cooling due to the formation of the Antarctic bottom water. Thus the stratification of the deeper layer of the model ocean remains unchanged, preventing the activation of the THC.

These results differ from what *Schiller et al.* [1996] found using a coupled ocean-atmosphere model developed at the Max-Planck-Institute (MPI) in Hamburg, Germany. In response to the input of a massive amount of freshwater, the THC of the MPI model collapsed into the completely inactive mode similar to what *Manabe and Stouffer* [1988] obtained. However, upon the termination of the freshwater discharge, the THC rapidly reintensifies, eventually regaining its original intensity, in sharp contrast to the behavior of the inactive mode obtained by *Manabe and Stouffer* [1988].

Using somewhat simpler coupled models in which an energy balance model of the atmosphere is combined with a general circulation model of oceans, U. Mikolajewicz (unpublished manuscript, 1997) and *Fanning and Weaver* [1997] also induced the collapse of the THC by discharging a sufficient amount of freshwater into the North Atlantic Ocean. After the termination of the freshwater discharge, the THC in their models remains at the inactive state and fails to reintensify. However, when the wind stress feedback process [e.g., *Weaver et al.*, 1993] is incorporated in their models, the THC recovered with a millennium timescale.

These results suggest that the state of the inactive THC is not a stable equilibrium. In order to pinpoint the specific causes for the difference in behavior between Manabe and Stouffer's and other models, it is necessary to conduct comparative assessment of relevant factors such as vertical diapycnal diffusion, the Antarctic bottom water formation, and the wind stress feedback in these models. Nevertheless, based upon the paleoceanographic evidences mentioned earlier, we suspect that the states of the Y-D and LGM oceans differ from

the state of inactive THC which *Manabe and Stouffer* [1988] and others induced by massive freshwater discharge. Instead, they resemble the state of the temporarily weakened THC obtained in the present FWN experiment.

The results obtained here could be relevant to the future change of climate. The recent study of *Manabe and Stouffer* [1993, 1994] reveals that associated with the CO_2-induced warming of the model atmosphere, the poleward transport of water vapor increases, causing marked increase in precipitation, and accordingly, increased freshwater supply in high latitudes. The simulated weakening of the THC in response to the doubling of atmospheric CO_2 resembles the response to the high-latitude discharge of freshwater described here. Because of the weakening, the northward advection of warm, saline surface water is reduced, moderating the warming in the northern North Atlantic and surrounding regions. In order to detect the future change in the intensity of the THC, it is urgent to monitor the structure of water mass in not only the North Atlantic but also the Arctic Ocean and Nordic Seas.

Acknowledgments. We are very grateful to T.P. Guilderson and R.G. Fairbanks, who generously shared with us the results from their analysis of high-resolution Barbados time series of [Sr/Ca] temperature and sea level prior to the publication. Thanks are also due to M.L. Bender, P.J. Fawcett, T.M. Hughes, J.D. Mahlman, E. Tziperman, A.J. Weaver, and M. Winton, who reviewed the paper and made valuable comments.

References

Bard, E., B. Hamelin, M. Arnold, L. Montaggioni, G. Cabioch, G. Faure, and F. Rougerie, Deglacial sea-level record from Tahiti corals and the timing of global meltwater discharge, *Nature, 382*, 241-244, 1996.

Basher, L.R., and M.J. McSaveney, An early Aranuian glacial advance at Cropp River, Central Westland, New Zealand, *J. R. Soc. N. Z., 19*, 263-268, 1989.

Bond, G., et al., Evidence for massive discharges of icebergs into the North Atlantic Ocean during the last glacial period, *Nature, 360*, 245-249, 1992.

Boyle, E.A., and L.D. Keigwin, North Atlantic thermohaline circulation during the past 20,000 years linked to high-latitude surface temperature, *Nature, 330*, 35-40, 1987.

Broecker, W.S., *The Glacial World According to Wally*, 318 pp. + appendix, Lamont-Doherty Earth Obs., Palisades, N.Y., 1995.

Broecker, W.S., D. Peteet, and D. Rind, Does the ocean-atmosphere system have more than one stable mode of operation?, *Nature, 315*, 21-25, 1985.

Broecker, W.S., M. Andree, W. Wolli, H. Oeschger, G. Bonani, J. Kennett, and D. Peteet, A case in support of a meltwater diversion as the trigger for the onset of the Younger Dryas, *Paleoceanography, 3*, 1-19, 1988.

Bryan, K., Climate and the ocean circulation, II, The ocean model, *Mon. Weather Rev., 97*, 806-827, 1969.

Bryan, K., and M. Cox, A numerical integration of the oceanic general circulation model, *Tellus, 19*, 54-80, 1967.

Bryan, K., and L. Lewis, A water mass model of the world ocean, *J. Geophys. Res., 84*(C5), 2503-2517, 1979.

Chappellaz, J., T. Blunler, D. Raynaud, J.M. Barnola, J. Schwander, and B. Stauffer, Synchronous changes in atmospheric CH_4 and Greenland climate between 40 and 80 K yr BP, *Nature, 366*, 443-445, 1993.

Clark, P.U., R.B. Alley, L.D. Keigwin, J.M. Licciardi, S.J. Johnsen, and H. Wang, Origin of the first meltwater pulse following the last glacial maximum, *Paleoceanography, 11*(5), 563-577, 1996.

Delworth, T.L., S. Manabe, and R.J. Stouffer, Interdecadal variation of the thermohaline circulation in a coupled ocean-atmosphere model, *J. Clim., 6*, 1993-2011, 1993.

Delworth, T.L., S. Manabe, and R.J. Stouffer, Multidecadal variability in the Greenland Sea and surrounding regions: a coupled model simulation, *Geophys. Res. Lett.*, in press, 1997.

Denton, G.H., and C.H. Hendy, Documentation of an advance of New Zealand's Franz Joseph Glacier at the onset of Younger Dryas time, *Science, 264*, 1434-1437, 1994.

Duplessy, J.-C., N.J. Shackleton, R.G. Fairbanks, L. Labeyrie, D. Oppo, and N. Kallel, Deep-water source variations during the last climate cycle and their impact on the global deepwater circulation, *Paleoceanography, 3*, 343-360, 1988.

Engstrom, D.R., B.C.S. Hansen, and H.E. Wright, Evidence in support of a Younger Dryas cooling in Alaska, *Science, 250*, 1383-1385, 1990.

Fairbanks, R.G., A 17,000 year glacio-eustatic sea level record: Influence of glacial melting rates on the Younger Dryas event and deep-ocean circulation, *Nature, 342*, 637-642, 1989.

Fairbanks, R.G., C.D. Charles, and J.D. Wright, Origin of global meltwater pulses, in *Radiocarbon After Four Decades*, edited by R.E. Taylor et al., pp. 473-500, Springer-Verlag, New York, 1992.

Fanning, A.F., and A.J. Weaver, Deglacial meltwater episodes: A simulation of the Younger Dryas, *Paleoceanography*, in press, 1997.

Gordon, C.T., and W. Stern, A description of the GFDL global spectral model, *Mon. Weather Rev., 110*, 625-644, 1982.

GRIP Members, Climate instability during the last interglacial period recorded in the GRIP ice core, *Nature, 364*, 203-207, 1993.

Guilderson, T.P., Tropical Atlantic SSTs over the last 20,000 yrs: Implications on the mechanism and synchroneity of climate change, Ph.D. thesis, Dep. of Earth and Environ. Sci., Columbia Univ., New York, 1996.

Guilderson, T.P., R.G. Fairbanks, and J.L. Rubenstone, Tropical temperature variations since 20,000 years ago: Modulating interhemispheric climate change, *Science, 263*, 663-665, 1994.

Haney, R.L., Surface thermal boundary condition for ocean circulation models, *J. Phys. Oceanogr., 1*, 241-248, 1971.

Hansel, A.K., and D.M. Michelson, A reevaluation of the timing and causes of high lake phases in the Lake Michigan basin, *Quat. Res., 29*, 113-128, 1988.

Jouzel, J., et al., The two-step shape and timing of the last deglaciation in Antarctica, *Clim. Dyn., 11*, 151-161, 1995.

Karpuz, N.A., and E. Jansen, A high-resolution diatom record of the last deglaciation from the SE Norwegian Sea: Documentation of rapid climatic changes, *Paleoceanography, 7*, 499-520, 1992.

Keigwin, L.D., and G.A. Jones, Glacial-Holocene stratigraphy, chronology and paleoceanographic observations on some North Atlantic sediment drift, *Deep Sea Res., 36*, 845-867, 1989.

Keigwin, L.D., and S.J. Lehman, Deep circulation linked to Heinrich event 1 and Younger Dryas in a middepth North Atlantic core, *Paleoceanography, 9*, 185-194, 1994.

Keigwin, L.D., G.A. Jones, and S.J. Lehman, Deglacial meltwater discharge, North Atlantic deep circulation, and abrupt climate change, *J. Geophys. Res., 96*(C9), 16,811-16,826, 1991.

Maier-Reimer, E., and U. Mikolajewicz, Experiments with an OGCM on the cause of the Younger Dryas, *Proc. Joint Oceanogr. Assem.*, 87-99, 1989.

Manabe, S., and R.J. Stouffer, Two stable equilibria of a coupled ocean-atmosphere model, *J. Clim., 1*, 841-866, 1988.

Manabe, S., and R.J. Stouffer, Century-scale effects of increased atmospheric CO_2 on the ocean-atmosphere system, *Nature, 364*, 215-218, 1993.

Manabe, S., and R.J. Stouffer, Multiple-century response of a coupled ocean-atmosphere model to an increase of atmospheric carbon dioxide, *J. Clim., 7*, 5-23, 1994.

Manabe, S., and R.J. Stouffer, Simulation of abrupt climate change induced by freshwater input to the North Atlantic Ocean, *Nature, 378*, 165-167, 1995.

Manabe, S., J. Smagorinsky, and R.F. Strickler, Simulated climatology of general circulation model with a hydrologic cycle, *Mon. Weather Rev., 93*, 769-798, 1965.

Manabe, S., R.J. Stouffer, M.J. Spelman, and K. Bryan, Transient

response of a coupled ocean-atmosphere model to gradual changes of atmospheric CO_2, I, Annual mean response, *J. Clim.*, *4*, 785-818, 1991.

Manabe, S., M.J. Spelman, and R.J. Stouffer, Transient response of a coupled ocean-atmosphere model to gradual changes of atmospheric CO_2, II, Seasonal response, *J. Clim.*, *5*, 105-126, 1992.

Marotzke, J., Instability and multiple equilibria of the thermohaline circulation, Ph.D. thesis, 126 pp., Christian-Albrecht Univ., Kiel, Germany, 1990.

Mathews, R.W., L.E. Heusser, and R.T. Patterson, Pollen-based evidence for a Younger Dryas cooling in British Columbia, *Geology*, *21*, 101-104, 1993.

Mayewski, P.A., et al., Climate change during the last deglaciation in Antarctica, *Science*, *272*, 1636-1638, 1996.

Orszag, S.A., Transform method for calculating vector-coupled sums: Application to the spectral form of the vorticity equation, *J. Atmos. Sci.*, *27*, 890-895, 1970.

Peteet, D., Global Younger Dryas?, *Quat. Int.*, *28*, 93-104, 1995.

Rahmstorf, S., Rapid climate transitions in a coupled ocean-atmosphere model, *Nature*, *372*, 82-85, 1994.

Rahmstorf, S., Bifurcations of the Atlantic thermohaline circulation in response to changes in hydrologic cycle, *Nature*, *378*, 145-149, 1995.

Rahmstorf, S., and J. Willebrand, The role of temperature feedback in stabilizing the thermohaline circulation, *J. Phys. Oceanogr.*, *25*, 788-805, 1995.

Redi, M.H., Oceanic isopycnal mixing by coordinate rotation, *J. Phys. Oceanogr.*, *12*, 1154-1158, 1982.

Sarnthein, M., K. Winn, S.A. Jung, J.-C. Duplessy, L. Labeyrie, H. Erlenkeuser, and G. Gaussen, Changes in east Atlantic deep water circulation over the past 30,000 years: Eight times slice reconstructions, *Paleoceanography*, *9*, 209-267, 1994.

Schiller, A., U. Mikolajewicz, and R. Voss, The stability of the thermohaline circulation in a coupled ocean-atmosphere general circulation model, *Rep. 188*, 42 pp., Max-Planck-Inst. for Meteorol., Hamburg, Germany, 1996.

Sowers, T., and M. Bender, Climate records covering the last deglaciation, *Science*, *269*, 210-213, 1995.

Stouffer, R.J., S. Manabe, M.J. Spelman, and K. Bryan, Interhemispheric asymmetry in climate response to a gradual increase of atmospheric CO_2, *Nature*, *342*, 660-662, 1989.

Thompson, L.G., E. Moseley-Thompson, M.E. Davis, P.-N. Lin, K.A. Henderson, J. Cole-Dai, J.F. Bolzan, and K.-B. Liu, Late glacial stage and Holocene tropical ice core records from Huascarán, Peru, *Science*, *269*, 46-50, 1995.

Tziperman, E., and K. Bryan, Estimating global air-sea fluxes from surface properties and from climatological flux data using an oceanic general circulation model, *J. Geophys. Res.*, *98*(C12), 22,629-22,644, 1993.

Weaver, A.J., and E.S. Sarachik, The role of mixed boundary conditions in numerical models of the ocean's climate, *J. Phys. Oceanogr.*, *21*, 1470-1493, 1991.

Weaver, A.J., J. Marotzke, P.F. Cummins, and E.S. Sarachik, Stability and variability of the thermohaline circulation, *J. Phys. Oceanogr.*, *23*, 1470-1493, 1993.

Winton, M., The effect of cold climate upon North Atlantic deep water formation in a simple ocean-atmosphere model, *J. Clim.*, in press, 1996.

Zhang, S., R.J. Greatbatch, and C.A. Lin, A reexamination of the polar halocline catastrophe and implications for coupled ocean-atmosphere modeling, *J. Phys. Oceanogr.*, *23*, 287-299, 1993.

S. Manabe and R.J. Stouffer, NOAA Geophysical Fluid Dynamics Laboratory, Princeton University, P.O. Box 308, Princeton, NJ 08542. (e-mail: sm@gfdl.gov; rjs@gfdl.gov)

(Received August 29, 1996; revised December 6, 1996; accepted December 19, 1996.)